



A Human Thermal Comfort Level Estimating Method Using Thermal Image and Sensor Data

Mao, Haomin ; Tsuchida, Shuhei ; Suzuki, Yuma ; Kim, Yongbeom ; Kanada, Rintaro ; Hori, Takayuki ; Terada, Tsutomu ; Tsukamoto, Masahiko

(Citation)

iiWAS2021: The 23rd International Conference on Information Integration and Web Intelligence:580-585

(Issue Date)

2021-12-30

(Resource Type)

conference paper

(Version)

Accepted Manuscript

(Rights)

© 2021 ACM

(URL)

<https://hdl.handle.net/20.500.14094/0100477536>



A Human Thermal Comfort Level Estimating Method Using Thermal Image and Sensor Data

HAOMIN MAO, Graduate School of Engineering, Kobe University, Japan

SHUHEI TSUCHIDA, Graduate School of Engineering, Kobe University, Japan

YUMA SUZUKI, SoftBank Corp., Japan

YONGBEOM KIM, SoftBank Corp., Japan

RINTARO KANADA, SoftBank Corp., Japan

TAKAYUKI HORI, SoftBank Corp., Japan

TSUTOMU TERADA, Graduate School of Engineering, Kobe University, Japan

MASAHIKO TSUKAMOTO, Graduate School of Engineering, Kobe University, Japan

Recently, it has become a trend to construct a thermal environment with human thermal comfort. The advantage of human thermal comfort is that we could adjust the environment through the thermal sensation of human. Since human thermal comfort is influenced by several factors such as environmental temperature, environmental humidity, airflow, mean radiant heat, and so on, it is usually difficult to be directly evaluated. This paper proposes a method of estimating subjective thermal comfort and objective thermal comfort using CNN by RGB image data, thermal image data, and sensor data. We built a pipe-type booth in a room with a small air conditioner, two heaters, a humidifier, and a dehumidifier to acquire learning data, and we trained CNN under six different learning patterns to estimate thermal comfort. We found that image data is conducive to estimate subjective thermal comfort, and sensor data is conducive to estimating objective thermal comfort.

CCS Concepts: • **Human-centered computing** → *Ubiquitous and mobile computing design and evaluation methods*.

ACM Reference Format:

HAOMIN MAO, SHUHEI TSUCHIDA, YUMA SUZUKI, YONGBEOM KIM, RINTARO KANADA, TAKAYUKI HORI, TSUTOMU TERADA, and MASAHIKO TSUKAMOTO. 2018. A Human Thermal Comfort Level Estimating Method Using Thermal Image and Sensor Data. In . ACM, New York, NY, USA, 8 pages. <https://doi.org/10.1145/1122445.1122456>

1 INTRODUCTION

Human thermal comfort is defined as a human's psychological satisfaction with the current thermal environment by American Society of Heating, Refrigerating and Air-Conditioning Engineers (ASHRAE) [1]. In an indoor environment, this satisfaction could be evaluated by the PMV model which is proposed by Fanger in 1970 [2]. PMV model, as shown in Table 1, claims the human's thermal sensation is expressed to a 7-level scale from -3 to 3. The positive scale indicates the level of human discomfort to the heat of indoor environment, and the negative scale indicates the level of human discomfort to the cold of indoor environment. The Neutral level means that the person in a room is comfortable. However, human thermal comfort could be divided into subjective thermal comfort and objective thermal comfort according to the acquisition method. The subjective thermal comfort is obtained by answering a questionnaire about

Permission to make digital or hard copies of all or part of this work for personal or classroom use is granted without fee provided that copies are not made or distributed for profit or commercial advantage and that copies bear this notice and the full citation on the first page. Copyrights for components of this work owned by others than ACM must be honored. Abstracting with credit is permitted. To copy otherwise, or republish, to post on servers or to redistribute to lists, requires prior specific permission and/or a fee. Request permissions from permissions@acm.org.

© 2018 Association for Computing Machinery.

Manuscript submitted to ACM

the current thermal sensation. On the other hand, the objective thermal comfort is calculated by the PMV formula from six parameters: metabolic rate, clothing insulation, mean radiation temperature, mean wind velocity, indoor mean temperature, and indoor relative mean humidity.

An ideal thermal environment is an environment in which the factors such as environmental temperature and environmental humidity could automatically adjust along with the human thermal comfort. In order to construct a thermal environment such as a smart room or smart office, it is essential to estimate human thermal comfort appropriately. It seems to be able to do estimation from wearable sensor data and environment sensor data easily. However, it might cause a problem in daily life that the user usually answers the subjective thermal comfort by the questionnaire and that it usually wears a large number of sensors on the body for calculating the objective thermal comfort. Considering the convenience of utilization in daily life, we presented two methods of estimating human thermal comfort: using a small number of wearable sensors and using cameras. Since estimating human thermal comfort with a small number of wearable sensors has already been proposed in the reference [3], we only discuss the method with cameras in this paper.

With rapid development in the computer vision field, it is possible to recognize a target from the image data using deep learning models more accurately. Significantly, the convolutional neural network (CNN) was noticed by researchers; AlexNet, VGG, ResNet, DenseNet were proposed successively after LeNet [4]. This paper presented a method to estimate subjective thermal comfort and objective thermal comfort through image data processed by the CNN model. And, since wearable sensors and environmental sensors are helpful for the estimation of human thermal comfort [3], we also verified how sensor data improves the estimation accuracy of human thermal comfort.

2 RELATED RESEARCH

Because thermal manikin could simulate human's thermal characteristics in the condition of wearing clothes, it has been widely used to evaluate the thermal environment in the past [5]. And, it is possible to calculate objective thermal comfort by controlling skin surface temperature of thermal manikin [6]. As image processing technology getting mature, a non-contact measurement method using thermal image was proposed. However, the parameters of PMV model cannot be acquired from thermal image. Gradually, the acquisition of human thermal comfort has been changed from calculating human thermal comfort to estimating human thermal comfort. For example, Ghahramani et al. developed a monitoring system of human thermal comfort with infrared thermography of the face [7]. Besides, machine learning is also applied to estimation. Li et al. collected temperature data of different parts of face from thermography, and estimated thermal comfort by letting Random Forest learn the combinations of the temperature of different parts of face [8]. Burzo et al. extracted the features from thermography by k-means and estimated human thermal comfort of a three-level scale of "hot," "neutral," and "cold" in three models of Decision Tree, k-NN, and Simple Bayes [9]. And in recent research, Maia et al. predicted horse thermal comfort to two class of "comfort" and "discomfort" by machine learning [10].

3 PROPOSED METHOD

This paper proposed a CNN model to estimate the human thermal comfort in an indoor environment. We acquired the RGB image data, thermal image data, and sensor data that could reflect the biological information of the human body as the learning data of the model. We also gathered correct labels of subjective thermal comfort data and objective thermal comfort data. And a pre-learning model, ResNet50, was used to extract features from the image data.

3.1 Acquisition of Learning Data

The RGB images for learning data are acquired by a webcam of Logicoool Co Ltd., and the thermal images are acquired by Lepton module of FLIR Systems Inc. In general, training CNN model requires a large amount of image data. For example, the first CNN model, LeNet, was trained 60 thousand handwritten number images [11]. One of the most famous CNN models, ResNet, used approximately 1.28 million images [12]. In this study, it is impossible to acquire such enormous image data, so data augmentation is carried out for increasing image data. There are mainly three sorts of data augmentation for images: affine transformation, RGB conversion, and noise injection [13]. Since RGB conversion cannot be used for thermal images, Reflection, Translation, and Gaussian Noise Injection were chosen for making the augmented images. The instance of the augmented images is shown in Figure 7.

As for sensor data, we used NTC thermistors, heart rate sensor, temperature and humidity sensor, and wind velocity sensor to acquire skin surface temperature (4 places of human body), heart rate, environmental temperature, environmental humidity, and mean wind velocity. Considering that the individual differences would affect human thermal comfort, BMR (basic metabolic rate), calculated by four data (weight, height, age, sex), was added to the learning data. Since the quantity of features of the sensor data is less than the image data, we calculated the mean value and variance value of 10 samples of data (about 3 minutes) before the measurement time for all sensor data, and adds them to the learning data set at measurement time. Thus, features of learning data of sensor data are extended from 12 dimensions to 30 dimensions.

3.2 Acquisition of Correct Labels of Subjective Thermal Comfort

Correct labels of the subjective thermal comfort are acquired from the answers of a thermal comfort questionnaire. However, since most people do not know the word "human thermal comfort," when they are asked: "What is your level of human thermal comfort?" it seems a bit difficult to answer. In contrast, the question "How many degrees do you want to increase or decrease about current room temperature?" could be understood even if people do not know about human thermal comfort or the PMV model. By setting seven options of this question from -3 to 3, the answer could correspond to the 7-level scale of the PMV model. We also developed an interface with Tkinter, a python library, to obtain the answers of this question in real-time during the experiment. The screenshot of the interface which is named as "PMV Questionnaire" is shown in Figure 1. The answer would be selected by experiment's participants in the check box next to "The Temperature Degrees Desiring to Change."

3.3 Acquisition of Correct Labels of Objective Thermal Comfort

Correct labels of objective thermal comfort are calculated by PMV formula. PMV formula is given by Equation 1:

$$\begin{aligned}
 PMV = & [0.303 * e^{-0.036M} + 0.028][(M - W) - 3.05 * 10^{-3}[5733 - 6.99(M - W) - P_a] \\
 & - 0.42[(M - W) - 58.15] - 1.7 * 10^{-5}M(5867 - P_a) - 0.0014M(34 - t_a) - 3.96 * 10^{-8} \\
 & f_{cl}[(t_{cl} + 273)^4 - (t_r + 273)^4] - f_{cl}h_c(t_{cl} - t_a)] \quad (1)
 \end{aligned}$$

where M is metabolic heat production, W is external mechanical work of human (generally 0), P_a is atmospheric pressure, t_a is environmental temperature, RH is the relative environmental humidity, f_{cl} is the clothing area factor, t_{cl} is the surface temperature of clothing, t_r is the mean radiation temperature, and h_c is the thermal convection coefficient. M is generally described as Mets, and 1 Mets could be converted to $58.2W/m^2$ heat. P_a is calculated by

Fig. 1. PMV Questionnaire Interface

Equation 2:

$$P_a = (RH/100 * e^{-(18.6686-4030.18/(t_a+235))}) \quad (2)$$

where RH is the the relative environmental humidity. t_a and RH could be measured by temperature and humidity sensor. f_{cl} is given by Equation 3:

$$f_{cl} = \begin{cases} 1.00 + 1.29 * I_{cl} (if I_{cl} \leq 0.078m^2k/w) \\ 1.05 + 0.645 * I_{cl} (if I_{cl} > 0.078m^2k/w) \end{cases} \quad (3)$$

where I_{cl} is the insulation of the clothing ensemble. I_{cl} is generally written in the form of clo value, where 1 clo could be converted to $0.0155m^2k/w$. t_{cl} is given by Equation 4:

$$t_{cl} = 35.7 - 0.028 * M - I_{cl} * [3.96 * 10^{-8} f_{cl} [(t_{cl} + 273)^4 - (t_r + 273)^4] - f_{cl} h_c (t_{cl} - t_a)] \quad (4)$$

Unlike to other equations, when we input other parameters in Equation 4, we would obtain a one-variable quartic equation, and t_{cl} is the solution of the equation. In order to simplify the calculation, we directly measured t_{cl} with an NTC thermistor. t_r is the median of the background temperature of thermal image. h_c is given by Equation 5:

$$h_c = \begin{cases} 2.38 * (t_{cl} - t_a)^{0.25} (if 2.38 * (t_{cl} - t_a)^{0.25} > 12.1(v_{ar})^{0.5}) \\ 12.1(v_{ar})^{0.5} * v_{ar} (if 2.38 * (t_{cl} - t_a)^{0.25} < 12.1(v_{ar})^{0.5}) \end{cases} \quad (5)$$

where v_{ar} is the mean wind velocity. And, v_{ar} is measured by wind sensor.

3.4 CNN Approach

The structure of the CNN model for learning image data and sensor data is shown in Figure 2. The structure of the CNN model for only learning image data is shown in Figure 3. In the two models, RGB image data and thermal image data are transformed to the shape of $3 \times 224 \times 224$ and input to ResNet50 in convolution layers. As the output of convolution layers, RGB image data and thermal image data are extracted as the features of the shape of $7 \times 7 \times 2048$, respectively. The outputs are connected and goes to global average pooling layer. Then, image data are output as the features of the shape of $1 \times 1 \times 4096$. So far, the two models have the same structure, but there will be some differences afterwards. In order to combine image data features and sensor data features, we used two fully connected layers in Figure 2. The fully connected layer 1 learns the features of image data and yields an 1×30 output. The fully connected layer 2 learns the output of fully connected layer 1 and sensor data features and outputs the final result(human thermal comfort). Since the model in Figure 3 does not need to correspond to sensor data input, it just used one fully connected layer to output the final result.

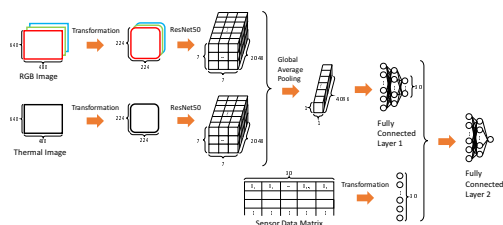


Fig. 2. CNN Structure While Estimating Thermal Comfort Using Image Data and Sensor Data

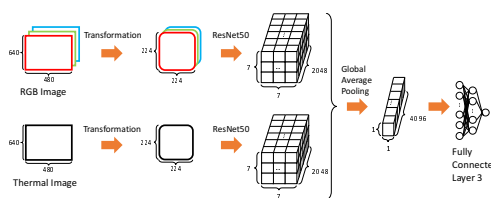


Fig. 3. CNN Structure While Estimating Thermal Comfort Using Image Data

Table 1. 7-Level Scale of PMV Model

Scale	Language Expression
+3	Hot
+2	Warm
+1	Slightly warm
0	Neutral
-1	Slightly cool
-2	Cool
-3	Cold

Table 2. Learning Pattern

Learning Pattern	Leaning Data	Correct Label
Pattern 1	Image Data and Sensor Data	7-Level Answered PMV
Pattern 2	Image Data	7-Level Answered PMV
Pattern 3	Image Data and Sensor Data	3-Level Answered PMV
Pattern 4	Image Data	3-Level Answered PMV
Pattern 5	Image Data and Sensor Data	Calculated PMV
Pattern 6	Image Data	Calculated PMV

3.5 Learning Patterns

In this paper, there are two configurations of learning data: image data and sensor data, image data only; the correct label of human thermal comfort has two forms: 7-level answered PMV value and calculated PMV value; therefore, four learning patterns could be compounded from learning data and the correct labels. If the environmental conditions are difficult to control, we may not be able to divide the thermal comfort into 7 levels. In this case, it is impossible to estimate the 7-level answered PMV value correctly. As a reference, we added a 3-level answered PMV value label to the correct label of subjective thermal comfort. The 3-level answered PMV value could simplify the expression of thermal comfort to cold, neutral and hot. Specifically, we converted the positive scale of the PMV model to 3 and the negative scale to -3 . Then, we obtained six learning patterns, as shown in Table 2.

4 EXPERIMENT

4.1 Experimental Environment

In order to acquire to data conveniently, we build a $1.5\text{m} \times 1.5\text{m} \times 2.0\text{m}$ pipe-type booth, in which two heaters, a cooler, a humidifier, and a dehumidifier were put, shown as Figure 4. This helps us to obtain data fastly on various environmental conditions. RGB camera and thermal camera are installed in front of where the participant sits. A temperature and humidity sensor and a wind sensor are fixed on a table with tape. The participants, who are attached with NTC thermistors at 5 locations(left leg, right leg, left arm, right arm, right thigh) and a heart beat sensor at right hand's little finger, will be asked to stay in the booth when image data and sensor data is acquired. Participants could choose an activity during the experiment, while the environmental temperature and humidity are constantly changed. The location of the cameras, environmental sensors and wearable sensors are shown in Figure 5.

Cooler, heater, humidifier, and dehumidifier have only two output modes respectively: on and off. So the environment controls in this paper is roughly divided into four situations: simultaneous turning heater and humidifier on, simultaneous turning heater and dehumidifier on, simultaneous turning cooler and humidifier on, and simultaneous turning cooler and dehumidifier on.

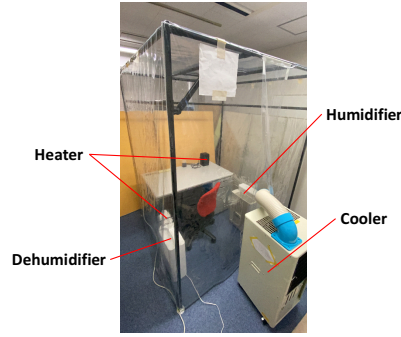


Fig. 4. Experimental Environment

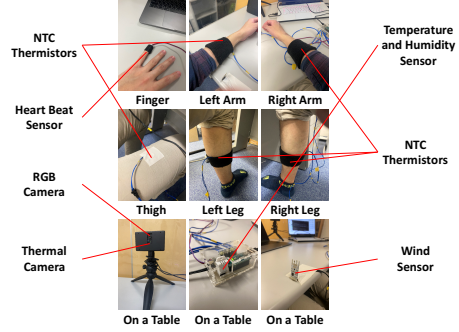


Fig. 5. The Locations of Wearable sensors, environmental sensors, and cameras

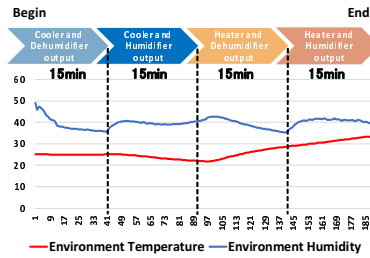


Fig. 6. Changes of the Environmental Temperature and Environmental Humidity in the Experiment of a Participant

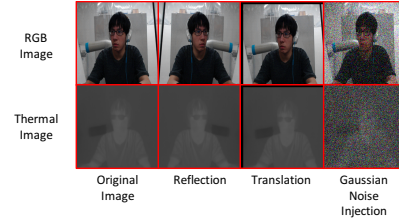


Fig. 7. Instance of Data Augmentation

4.2 Experiment Description

The participants will be asked to rest for 10 minutes before the experiment start, and during this time they could fill their name, private information, Mets, clo value, the degree of temperature desiring to change in PMV questionnaire interface. Mets and Clo value could be referred to the energy expenditure of the activities table and the guideline for clo value [15–18]. However, participants are not allowed to change their activity and clothes during the experiment.

Since it takes time when the temperature and humidity in the booth being stable, the measurement time for each pattern is set to 15 minutes, and image data and sensor data was acquired at 20-second intervals during that time. Corresponding to four situations of environment controls, four measurements will be conducted during experiment. Figure 6 shows changes of the environmental temperature and environmental humidity in the experiment of a participant.

In the experiment, if participant wants to change the current environmental temperature, he or she can change the option of "The Degree of Temperature Desiring to Change" field of interface, though the temperature will not be modified. Above all, it usually takes one and a half hours for each participant including resting time, explanation time for experiment, and experiment time. We obtained data from 11 participants in this paper. After the measurement, the outliers and the other sensor data simultaneously with the outlier were removed from the acquired data set.

4.3 Learning Requirement

We obtained 1605 data from 11 participants, of which 60% were used as training data, 20% were used as validation data, and 20% were used as test data. The training data can be increased to 3728 sets of data after data augmentation. Even if 3728 images still do not reach the mounts of training data used in Reference [12], we used transfer learning.

Table 3. Performance Metrics Using ResNet50

Learning Pattern	Test MAE	Test F1 Score
Pattern 1	1.04	0.42
Pattern 2	0.90	0.45
Pattern 3	0.85	0.76
Pattern 4	0.60	0.80

Learning Pattern	Test MAE	Test RMSE
Pattern 5	1.19	2.04
Pattern 6	2.67	3.58

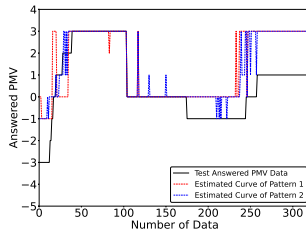


Fig. 8. Estimation Curve for 7-Level Answered PMV

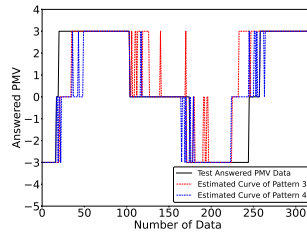


Fig. 9. Estimation Curve for 3-Level Answered PMV

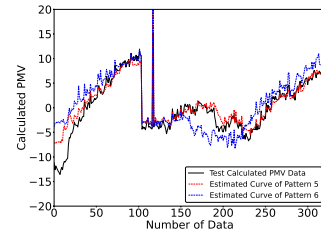


Fig. 10. Estimation Curve for Calculated Answered PMV

Concretely speaking, the original fully connected layers of ResNet50 were cut off, and the remaining weights were frozen [14]. That is, when training the model of Figure 2 with image data and sensor data, only the weights of Fully Connected Layer 1 and Fully Connected Layer 2 would be updated; and, when training the model of Figure 3 with image data, only the weights of Fully Connected Layer 3 would be updated. We also used early stopping to prevent overfitting of the CNN model. Early stopping is a technique that returns an epoch with the minimum validation error. We monitored Validation CEE(Cross Entropy Error) in Pattern 1 to Pattern 4 and Validation MSE(Mean Squared Error) Pattern 5 and Pattern 6. The value of patience for all learning patterns is set to 20 epochs.

5 ESTIMATION RESULT

The estimated results of subjective thermal comfort are shown in the upper half of Table 3. Figure 8 shows the estimated curves of the 7-level answered PMV value of subjective thermal comfort, and Figure 9 shows the estimated curves of the 3-level answered PMV value of subjective thermal comfort. In all subjective thermal comfort learning patterns, the estimation accuracy of Pattern 1 is the worst, and that of Pattern 4 is the best. Comparing Pattern 1 and 2 with Pattern 3 and 4, we could know that the estimation accuracy for the 3-level answered PMV is higher than the 7-level answered PMV. Moreover, the estimation accuracy is lower in the patterns using the sensor data from the comparison with Pattern 2 and 4. It seems that the utilization of the sensor data was ineffective for the improvement of estimation accuracy of the subjective thermal comfort. In Pattern 1 and 2, many labels of -1 and 1 were misestimated. We could see the misestimated parts from the 170th data to the 240th data and the 260th data to the 320th data in the estimated curves of Figure 8. Since the F1 score of Pattern 1 and 2 are lower than Pattern 3 and 4, it is necessary to improve the estimation accuracy by modifying the structure of the CNN model or learning condition.

The estimated results of objective thermal comfort are shown in the lower half of Table 3, and the estimated curves are shown in Figure 10. It seems that sensor data effectively improves the estimation accuracy of the objective thermal comfort because both Test MAE and Test RMSE of Pattern 5 are lower than that of Pattern 6. Though Test MAE of Pattern 5 and Pattern 6 are higher than that of Pattern 1 to Pattern 4, the estimation curves of Pattern 5 and Pattern 6 are more excellent by comparing Figure 8, Figure 9, and Figure 10. It is considered that the range of change of objective thermal comfort is broader than that of subjective thermal comfort. Moreover, since Pattern 5 and Pattern 6 are considerably adapted to the outliers, both of two patterns are a little overfitting.

6 CONCLUSION

This paper proposed an estimation method of subjective thermal comfort and objective thermal comfort in an indoor environment using RGB image data, thermal image data, and nine sorts of sensor data. In our proposed method, RGB images, thermal images, and sensor data were acquired by 11 participants in a specially prepared experimental room. From the estimated result, the estimation accuracy of the subjective thermal comfort for the 3-level answered PMV with the image data only is the highest. The estimation accuracy of the subjective thermal comfort for the 7-level answered PMV was the lowest with the image and sensor data. Image data played an important role in estimating subjective thermal comfort, and sensor data played an important role in estimating objective thermal comfort.

As our future work, the construction of the system that estimates human thermal comfort in the daily environment using the deep learning model will be considered to evaluate the estimation method. And we will consider how to estimate the human thermal comfort of multiple people in a room.

ACKNOWLEDGMENTS

This work is grateful to great assistance of Softbank Corp. and the cooperation of the experiment participants.

REFERENCES

- [1] N. Djongyang, R. Tchinda, D. Njomo: Thermal comfort: A review paper, *Journal of Renewable and sustainable energy reviews*, Vol. 14, No. 9, pp. 2626–2640 (Dec. 2010).
- [2] P. O. Fanger: Thermal Comfort. Analysis And Applications in Environmental Engineering, *Journal of Thermal Comfort. Analysis And Applications in Environmental Engineering*, pp. 244 (1970).
- [3] H. Mao, S. Tsuchida, Y. Kim, et. al.: A Thermal Comfort Estimation Method by Wearable Sensors, *Proceedings of the 36th Annual ACM Symposium on Applied Computing*, pp. 603–610 (Mar. 2021).
- [4] Z. Li, W. Yang, S. Peng, F. Liu: A Survey of Convolutional Neural Networks: Analysis, Applications, and Prospects, *Computing Research Repository*, pp. 1–21 (Apr. 2020).
- [5] H. Ingvar: Thermal manikin history and applications, *European Journal of Applied Physiology*, Vol. 92, No. 6, pp. 614–618 (June 2004).
- [6] S. Tanabe, E. A. Arens, F. Bauman, et. al.: Evaluating Thermal Environments by Using a Thermal Manikin with Controlled Skin Surface Temperature, *Ashrae Transactions*, Vol. 100, pp. 39–48 (Jan. 1994).
- [7] A. Ghahramani, G. Castro, B. Becerik-Gerber, et. al.: Infrared thermography of human face for monitoring thermoregulation performance and estimating personal thermal comfort, *Building and Environment*, Vol. 109, pp. 1–11 (Nov. 2016).
- [8] D. Li, C. C. Menassa, V. R. Kamat: Non-intrusive interpretation of human thermal comfort through analysis of facial infrared thermography Author links open overlay panel, *Energy and Buildings*, Vol. 176, pp. 246–261 (Oct. 2018).
- [9] M. Burzo, M. Abouelenien, V. Pérez-Rosas, et. al.: Using Infrared Thermography and Biosensors to Detect Thermal Discomfort in a Building's Inhabitants, *Proceedings of ASME 2014 International Mechanical Engineering Congress and Exposition*, Vol. 6B, No. 15, pp. 1–11 (Nov. 2014).
- [10] A. P. A. Maia, S. R. M. Oliveira, D. J. Moura, et. al.: A Decision-tree-based Model for Evaluating the Thermal Comfort of Horses, *Scientia Agricola*, Vol. 70, No. 6, pp. 377–383 (Nov. 2013).
- [11] Y. LeCun, L. Bottou, Y. Bengio, et. al.: Gradient-based Learning Applied to Document Recognition, *Journal of the IEEE*, Vol. 86, No. 11, pp. 2278–2324 (Nov. 1998).
- [12] K. He, X. Zhang, S. Ren, and J. Sun: Deep Residual Learning for Image Recognition, *Proceedings of the IEEE Conference on Computer Vision and Pattern Recognition*, pp.770–778 (June 2016).
- [13] S. Connor and T. M. Khoshgoftaar: A survey on Image Data Augmentation for Deep Learning, *Journal of Big Data*, Vol. 6, No. 60, pp. 1–48 (July 2019).
- [14] K. Weiss, T. M. Khoshgoftaar, and D. Wang: A Survey of Transfer Learning, *Journal of Big data*, Vol. 3, No. 9, pp. 1–40 (May 2016).
- [15] 2011 Compendium of Physical Activities, https://download.lww.com/wolterskluwer_vitalstream_com/PermaLink/MSS/A/MSS_43_8_2011_06_13_AINSWORTH_202093_SDC1.pdf.
- [16] Clo - Clothing and Thermal Insulation, https://www.engineeringtoolbox.com/clo-clothing-thermal-insulation-d_732.html.
- [17] M. Jette, K. Sidney, and G. Blümchen: Metabolic Equivalents (mets) in Exercise Testing, Exercise Prescription, and Evaluation of Functional Capacity, *Clinical cardiology*, Vol. 13, No. 8, pp. 555–565 (Aug. 1990).
- [18] E. A. McCullough, B. W. Jones, and J. Huck: A Comprehensive Data Base for Estimating Clothing Insulation, *Ashrae Trans*, Vol. 91, No. 2, pp. 29–47 (Aug. 1985).